Published in final edited form as:
Mol Carcinog. 2009 October ; 48(10): 873–885. doi:10.1002/mc.20527.

Targeted disruption of Bcl-x_L in mouse keratinocytes inhibits both UVB- and chemically-induced skin carcinogenesis

Dae Joon Kim, **Ken Kataoka**, **Shigetoshi Sano**[1], **Kevin Connolly**, **Kaoru Kiguchi**, and **John DiGiovanni**[*]

Department of Carcinogenesis, The University of Texas M.D. Anderson Cancer Center, Science Park-Research Division, Smithville, Texas, USA

[1]Department of Dermatology, Osaka University Graduate School of Medicine, Osaka, Japan

Abstract

Bcl-x_L is one of several antiapoptotic proteins regulated by signal transducer and activator of transcription 3 (Stat3). We have recently shown that Stat3 is required for chemically-induced and ultraviolet B (UVB)-induced skin carcinogenesis. In this study, the functional role of Bcl-x_L in skin carcinogenesis was investigated using skin-specific Bcl-x_L-deficient mice. In this model, Bcl-x_L expression is disrupted in the basal compartment of mouse epidermis using the bovine keratin 5 (K5) promoter to drive expression of *Cre* recombinase (K5.Cre × Bcl-$x_L^{fl/fl}$ mice). A significant increase in apoptosis induced by either UVB irradiation or 7,12-dimethylbenz[*a*]anthracene (DMBA) treatment was observed in the epidermis of Bcl-x_L-deficient mice. Furthermore, an increase in apoptotic cells was noted in hair follicle keratinocytes, including those located in the bulge region. Cell proliferation was not affected by Bcl-x_L deficiency following exposure to either UVB or 12-*O*-tetradecanoylphorbol-13-acetate (TPA). Bcl-x_L-deficient mice were more resistant than wild-type controls to skin tumor development with delayed onset and reduced number of tumors using either UVB or the DMBA/TPA two-stage regimen. Moreover, Bcl-2, Mcl-1, and survivin protein levels were increased in the epidermis of Bcl-x_L-deficient mice in the absence of stimuli. Furthermore, levels of these antiapoptotic proteins were also high in skin tumors from Bcl-x_L-deficient mice that developed in response to either UVB or two-stage carcinogenesis protocols. Collectively, these studies demonstrate that Bcl-x_L plays a role early in skin carcinogenesis through its anti-apoptotic functions to enhance survival of keratinocytes, including bulge region keratinocyte stem cells, following DNA damage.

Keywords

apoptosis; DMBA; TPA

Introduction

Apoptosis, a distinct form of programmed cell death, is a critical mechanism that eliminates unwanted and unnecessary cells without causing inflammation. It is involved in normal

[*]To whom correspondence should be addressed: John DiGiovanni, 1808 Park Road 1C, PO Box 389, Smithville, TX 78957, jdigiova@mdanderson.org, Tel: 512-237-9414, Fax: 512-237-2522.

physiological functions, development, differentiation, and the maintenance of tissue and organ homeostasis through tight regulation of cell turnover [1–4]. In addition, apoptosis plays an important role in removing damaged cells produced by exposure to environmental factors, such as ultraviolet (UV)-radiation and chemicals. Abnormalities in apoptotic cell death due to genetic defects and aberrant signaling pathways can lead to various diseases including cancer [5–7]. Members of the B-cell lymphoma-2 (Bcl-2) family of proteins are key regulators primarily of the intrinsic apoptotic pathways that regulate mitochondrial outer membrane permeabilization for cytochrome c release [3, 8]. There are approximately 20 members of the Bcl-2 family that are functionally either pro- or anti-apoptotic [4, 8]. Bcl-x_L is a Bcl-2 family member involved in maintaining cellular homeostasis through inhibition of both intrinsic and extrinsic apoptotic pathways [reviewed in 9].

Bcl-2 was the first proto-oncogene identified that derives its oncogenic activity by inhibiting cell death rather than by stimulating proliferation, and it is involved in various types of human cancer including prostate, lung, and skin cancers [9–12]. Inhibition of Bcl-2 has been shown to reduce tumor cell survival [13–16]. Studies of the role of Bcl-2 in skin carcinogenesis have produced conflicting results. In this regard, transgenic mice overexpressing Bcl-2 under the control of a human K1 promoter were more resistant to cell death induced by UVB irradiation and 7,12-dimethylbenz[*a*]anthracene (DMBA) treatment [17]. Furthermore, these mice developed papillomas with a significantly greater frequency and shorter latency compared with control littermates [17]. In contrast, transgenic mice overexpressing Bcl-2 under the control of a human K14 promoter were more resistant to both UVB- and chemically-induced skin carcinogenesis with skin tumor development occurring at a significantly lower frequency than control littermates [18].

Several studies have also revealed a significant role for Bcl-x_L in many human cancers [reviewed in 5, 9, 19–21]. In skin carcinogenesis, it is thought that Bcl-x_L is involved in the response of keratinocytes to both UV and chemical exposure as well as in skin tumor development [reviewed in 9]. For example, inhibition of Bcl-x_L by antisense oligonucleotides in human keratinocytes resulted in an increased sensitivity to apoptosis induced by UVB irradiation or cisplatinum treatment [22]. Further, this increased sensitivity in Bcl-x_L-deficient keratinocytes was enhanced by treatment with wortmannin, an inhibitor of phosphatidylinositol-3 kinase (PI3K), compared with wild-type keratinocytes [23], suggesting that cooperation between Bcl-x_L and PI3K-Akt signaling could enhance keratinocyte cell survival. Transgenic mice overexpressing Bcl-x_L under the control of the human K14 promoter were resistant to apoptosis induced by UVB irradiation compared with wild-type littermates [24]. These Bcl-x_L transgenic mice also developed a two-fold greater number of papillomas and developed invasive squamous cell carcinomas (SCCs) earlier and more frequently than control mice [25]. These studies suggested that inhibition of apoptosis through Bcl-x_L overexpression contributed to increased formation of skin tumors and possibly enhanced progression of these tumors [25].

Recently, our laboratory has shown that Stat3 deficiency leads to dramatic inhibition of both two-stage chemical carcinogenesis as well as UVB-induced carcinogenesis in mouse skin [26, 27]. Stat3 deficiency leads to increased apoptosis in keratinocytes in response to DNA damage induced by either DMBA or UVB, which contributes to decreased susceptibility to

skin carcinogenesis by these agents [26–28]. In addition, Stat3 is required for proliferation during the tumor promotion stage of skin carcinogenesis [26–28]. Bcl-x_L is a Stat3-regulated gene [29, 30] and levels of this protein are significantly reduced in keratinocytes of Stat3-deficient mice [27, 28, 31]. These data suggest that Bcl-x_L may mediate some of the effects of Stat3 during epithelial carcinogenesis. In the current studies, we investigated the functional role of Bcl-x_L in both two-stage chemical carcinogenesis and UVB-induced carcinogenesis in mouse skin using keratinocyte-specific Bcl-x_L-deficient mice. Through these studies, we provide direct evidence that Bcl-x_L is a critical antiapoptotic protein that contributes to the survival of DNA-damaged keratinocytes, including stem/progenitor cells located in hair follicles, during the initiation stage of skin carcinogenesis. In addition, the results suggest that Bcl-x_L may mediate some of the effects of Stat3 during epithelial carcinogenesis, again primarily during the initiation stage. Finally, upregulation of other antiapoptotic proteins (e.g., Bcl-2, mcl-1 and survivin) may partially compensate for loss of Bcl-x_L during skin carcinogenesis in skin specific Bcl-x_L-deficient mice.

Materials and methods

Generation of experimental animals

The generation and characterization of skin specific Bcl-x_L-deficient mice (K5.Cre × Bcl-$x_L^{fl/fl}$) has been previously described [23]. Bcl-$x_L^{fl/fl}$ mice were originally generated on a C57BL/6 genetic background. The Bcl-$x_L^{fl/fl}$ alleles were crossed for at least 10 generations onto the FVB/N genetic background. Female K5.Cre × Bcl-$x_L^{fl/fl}$ mice and non-transgenic littermates at 7–8 weeks of age were used for the described experiments. The dorsal skin of each mouse was shaved 48 hours before UVB irradiation or DMBA treatment; only those mice in the resting phase of the hair cycle were used. Newborn K5.Cre × Bcl-$x_L^{fl/fl}$ or wild-type littermates were used to generate primary cultures of mouse keratinocytes.

Keratinocyte culture and DMBA treatment *in vitro*

Primary cultures of keratinocytes were generated and cultured from wild-type and Bcl-x_L-deficient neonates as previously described [32] using keratinocyte growth medium (Cambrex Inc., Walkersville, MD). Two days after incubation (37°C, 5% CO_2), cells were 60 to 70% confluent, at which time they were treated with DMBA at a final concentration of 30 nM. After twelve hours of incubation, keratinocytes with morphological changes characteristic of apoptosis such as cell ballooning, nuclear condensation, and bleb formation were counted under a phase-contrast microscope as previously described [23]. Cells were counted from at least three nonoverlapping fields. The percentage of apoptotic cells was calculated as follows: [number of apoptotic cells/(number of apoptotic cells plus number of viable cells)] × 100.

RNA interference (RNAi) and apoptosis assay

Primary keratinocytes obtained from wild-type neonates were grown overnight to ~40% confluence and transfected with ON-TARGETplus SMART pool short interfering RNA (siRNA) specific for mouse Bcl-x_L or ON-TARGETplus siCONTROL non-targeting pool siRNA as a control (Dharmacon Inc., Layfayette, CO). Transfection was peformed with Lipofectamine RNAiMAX (Invitrogen, Carlsbad, CA). Forty-eight hours after siRNA

transfection, cells were irradiated with UVB at 800 J/m^2. Twelve hours later, apoptotic keratinocytes were detected using an In Situ Cell Death Detection Kit (Roche Diagnostics Co., Indianapolis, IN). Cells were counted microscopically in at least three nonoverlapping fields. The percentage of apoptotic cells was determined as described above.

UVB irradiation *in vivo*

Westinghouse FS20 sun lamp bulbs with a peak emission at 313 nm were used for UVB irradiation. The fluence rate was measured with an IL1400A Radiometer/Photometer coupled to a SEL240/UVB-1/TD detector (International Light, Inc., Newburyport, MA). Each mouse was held in individual compartments of a plastic cage on a rotating base to prevent any differences in fluence across the UV light bulbs. An UVB-transparent lid covering the radiation chamber was used to filter out the small amount of UVC radiation emitted from these lamps.

Flow cytometry

Primary keratinocytes were irradiated with UVB at 800 J/m^2 to analyze sub-G_1 DNA content by fluorescence-activated cell sorting (FACS). Twelve hours after UVB irradiation, cultured cells were harvested and fixed with 70% ethanol for 24 hours. The cells were suspended in 100 μl phosphate-citrate buffer for 30 minutes, washed, and suspended in a final volume of 0.3 mL of PBS. After the addition of propidium iodide (Calbiochem, San Diego, CA) and RNase (Sigma-Aldrich) to the cell suspensions, immunofluorescence was measured with a BD FACSAria Flow Cytometer (BD Biosciences, San Jose, CA). The percentage of cells below the G_1 peak (sub-G_1 fraction) was measured using Multicycle AV software (Phoenix Flow Systems, La Jolla, CA) to determine the apoptotic cell population.

Analysis of epidermal apoptosis following UVB irradiation or DMBA treatment

To analyze UVB-induced epidermal apoptosis, groups of mice (n = 3) were irradiated with UVB at 1,200 J/m^2 and sacrificed 24 or 48 hours after irradiation. Skin sections were stained with an antibody to the active form of caspase-3 (R&D Systems Inc.) and then treated with biotinylated anti-rabbit IgG and HRP-conjugated ABC reagent (BD Biosciences – Pharmingen, Los Angeles, CA). Apoptotic interfollicular and follicular keratinocytes were counted microscopically in at least three nonoverlapping fields in saggital sections from each mouse. To analyze DMBA-induced epidermal apoptosis, groups of mice (n = 3) were treated with a single application of DMBA (25, 100, or 1,000 nmol) or acetone, sacrificed 24 or 48 hours after treatment, and assessed as described above.

Immunohistochemistry of DNA photoproducts

Groups of mice (n = 3) were irradiated with UVB at 1,200 J/m^2 and sacrificed 24 or 48 hours after irradiation. After sacrifice, the dorsal skin was removed and fixed in 10% neutral-buffered formalin. To detect UVB-induced cyclobutane pyrimidine dimers (CPDs), skin sections were deparaffinized, rehydrated in xylene followed by graded ethanol (100%, 95%) and endogenous peroxidase activity was blocked with 3% hydrogen peroxide in water for 10 minutes. Skin sections were then boiled in 1 mM EDTA buffer (pH 8.0) for 10 minutes, cooled slowly, and preincubated for 10 minutes at room temperature with Biocare

blocking reagent (Biocare Medical Co., Concord, CA). Slides were incubated with primary mouse monoclonal CPD antibody (Kamiya Biomedical Co., Seattle, WA) at 1:80,000 dilution for 1 hour at room temperature followed by incubation with biotinylated rabbit anti-mouse antibody, streptavidin-horseradish peroxidase conjugate for detection, and developed with diaminobenzidine as a substrate. Photoproduct-positive keratinocytes were counted microscopically in at least three nonoverlapping fields in sections from each mouse and calculated as the percent of the number of photoproduct-positive cells/cm.

Confocal microscopy

Mice were irradiated with UVB at 1,200 J/m^2 and sacrificed 24 hours after irradiation. Skins were removed and fixed in formalin followed by embedding in paraffin. Skin sections were stained with K15 (Neomarkers Inc, Fremont, CA) and CD34 (BD Pharmingen, San Jose, CA) as described by Trempus *et al*. [33]. Skin sections were also stained with active caspase-3 (R&D Systems, Minneapolis, MN) antibodies as previously described [26, 27]. Alexa Fluor 488 goat anti-mouse IgG, Alexa Fluor 488 donkey anti-rat IgG and Alexa Fluor 594 goat anti-rabbit IgG (Invitrogen, Carlsbad, CA) were used as secondary antibodies for K15, CD34 and caspase-3, respectively. Slides were mounted using mounting medium with DAPI (Vector Laboratories, Inc., Burlingame, CA). Fluorescent images were then analyzed on a confocal microscope (Zeiss 510 META).

Analysis of epidermal thickness and cell proliferation following UVB irradiation or TPA treatment

To analyze UVB-induced epidermal thickness and cell proliferation, groups of mice (n = 3) were irradiated with UVB at 1,200 J/m^2 and sacrificed 24 or 48 hours after irradiation. Mice were injected intraperitoneally with 5-bromo-2-deoxyuridine (BrdU; Sigma-Aldrich, St. Louis, MO) at 100 μg/g body weight in PBS 30 minutes prior to sacrifice. Dorsal skin was then fixed in formalin and embedded in paraffin prior to sectioning of 4 μm and stained with hematoxylin and eosin. To determine epidermal cell proliferation, sections were stained with an anti-BrdU antibody (BD Biosciences – Pharmingen), followed by treatment with biotinylated anti-mouse IgG, and horseradish-peroxidase conjugated ABC reagent (Vector Laboratories). Epidermal cell proliferation (labeling index; LI), was determined as follows: A minimum of 500 basal cells was counted and calculated as the percent of the number of BrdU-positive cells/500 basal cells. Epidermal thickness was measured from 50 interfollicular sites per each group. To analyze TPA-induced epidermal thickness and cell proliferation, groups of mice (n = 3) were treated with a single application of TPA (6.8 nmol) or acetone, sacrificed 24 or 48 hours after treatment, and assessed as described above.

UV skin carcinogenesis

An incrementally graded UV protocol previously described [34] was modified and used to reduce ear papilloma formation. Bcl-x$_L$-deficient (K5.Cre × Bcl-x$_L^{fl/fl}$, n=11) and control (K5.Cre × Bcl-x$_L^{wt/wt}$, n=15) mice were exposed to 2,200 J/m^2 of UVB three times per week for weeks 1–6, 2,600 J/m^2 of UVB for weeks 7–8, 3,000 J/m^2 of UVB for weeks 9–10, 3,600 J/m^2 of UVB for weeks 11–12, 4,050 J/m^2 of UVB for weeks 13–14, and 4,500 J/m^2 of UVB for weeks 15–30. UVB irradiation was stopped at 31 weeks and mice were kept

without treatment until 43 weeks. Mice were monitored for tumor formation weekly. Skin tumors that developed on dorsal skin and ear were counted following the first tumor appearance. At the termination of the experiment, mice were sacrificed and tumors were collected for histopathologic evaluation and for Western blot analysis.

Two-stage skin carcinogenesis

Bcl-x_L-deficient (n=11) and wild-type littermates (n=11) were initiated with DMBA (25 nmol dissolved in 0.2 mL acetone; Sigma-Aldrich). Two weeks after DMBA treatment, mice were treated topically with TPA (6.8 nmol TPA dissolved in 0.2 mL acetone; LC Laboratories, Woburn, MA) twice a week for 21 weeks. Mice were monitored for tumor formation weekly. Skin tumors were counted following the first tumor appearance. Tumors were collected at the end of the study for histopathologic evaluation and for Western blot analysis.

Preparation of protein lysates and Western blot analysis

Preparation of protein lysates and Western blot analysis were performed as described previously [31].

Results

Bcl-x_L deficiency sensitizes epidermal keratinocytes to UVB-induced apoptosis

Previous studies showed that Bcl-x_L overexpression in the epidermis increased resistance to UVB-induced apoptosis [24]. To further investigate the role of Bcl-x_L in UVB-induced apoptosis, primary keratinocytes were transfected with 20 nM Bcl-x_L siRNA and then irradiated with UVB. The apoptotic response in cultured mouse keratinocytes transfected with Bcl-x_L siRNA was higher compared to keratinocytes transfected with mismatch control siRNA in the absence of UVB irradiation. Following UVB irradiation, keratinocytes transfected with Bcl-x_L siRNA showed a significant increase in apoptosis compared with keratinocytes transfected with control siRNA (Figure 1A). Furthermore, the number of apoptotic cells was significantly increased in cultured keratinocytes derived from Bcl-x_L-deficient mice following UVB irradiation compared with keratinocytes from wild-type mice (Figure 1B).

In addition to the studies using cultured keratinocytes, apoptosis was also evaluated in skin sections from UVB-irradiated mice. In this regard, caspase-3-positive cells in the epidermis of control and Bcl-x_L-deficient mice following UVB irradiation were observed in both the hair follicles as well as interfollicular epidermis. Figure 2A shows a representative caspase-3-stained section from Bcl-x_L-deficient mice following treatment with UVB. In this skin section, caspase-3 stained cells can be seen in the interfollicular epidermis (arrowheads) as well as the hair follicles (arrows). In the hair follicles of this section, the caspase-3 positive cells appear to be located either above the sebaceous glands or in the isthmus (below the sebaceous gland but above the bulge region). As shown in Figure 2B and 2C, the number of apoptotic cells was significantly increased in both interfollicular epidermis and hair follicles of Bcl-x_L-deficient mice following UVB irradiation compared with epidermis from wild-type mice. Note also that there was a much greater proportion of apoptotic cells

observed in the interfollicular epidermis compared to the follicular epidermis following UVB exposure in skin of both genotypes. Further analysis using confocal microscopy indicated that a proportion of caspase-3 positive cells observed in hair follicles also expressed K15, a marker for bulge region keratinocyte stem cells (KSCs). As shown in Figure 3A, in some cases the K15/caspase-3 positive cells appeared to be localized in the bulge region of hair follicles. In addition, some caspase-3 positive cells were positive for CD34 and also appeared to be localized in the bulge region (Figure 3B). Finally, some caspase-3 positive cells were clearly localized in the isthmus as noted above and did not stain positive for K15 (Figure 3C). Collectively, the data in Figures 2 and 3 suggest that Bcl-x_L protects keratinocytes, including stem/progenitor cell populations located in the hair follicles from UVB-induced apoptosis.

UVB exposure causes DNA damage and mutations in runs of tandemly located pyrimidine residues of DNA, and induces primarily cyclobutane pyrimidine dimers (CPDs) and pyrimidine (6-4) pyrimidone photoproducts (6-4 PPs) [35–37]. To examine whether Bcl-x_L plays a role specifically in the survival of photoproduct-positive cells following UVB irradiation, control and Bcl-x_L-deficient mice were irradiated with UVB and the CPD-positive cells in the epidermis and hair follicles were quantified. As shown in Figure 4, there was a decrease in CPD-containing cells in the interfollicular epidermis and hair follicles of both wild-type and Bcl-x_L-deficient mice 48 hours after UVB irradiation. Furthermore, there was a significantly greater decrease in CPD-positive cells in Bcl-x_L-deficient mice 48 hours after UVB exposure compared to wild-type mice. Although the data shown in Figure 4 represents the combined data for both the interfollicular epidermis and hair follicles, changes in the number of CPD containing cells in both compartments followed a similar pattern (data not shown). Thus, Bcl-x_L status *in vivo* influenced the survival of CPD-containing keratinocytes, which is consistent with the conclusion that Bcl-x_L influences survival of UV-photoproduct containing cells that arise shortly after exposure to UVB.

Bcl-x_L deficiency sensitizes epidermal keratinocytes to DMBA-induced apoptosis

Previous studies showed that overexpression of Bcl-x_L in mouse epidermis inhibited apoptotic cell death induced by DMBA [25]. To further investigate the role of Bcl-x_L in DMBA-induced apoptosis, primary keratinocytes from control and Bcl-x_L-deficient mice were treated with DMBA at a concentration of 30 nM. The number of apoptotic cells was significantly increased in Bcl-x_L-deficient keratinocytes compared with control keratinocytes after DMBA treatment (Figure 5A).

Similar to the results observed using cultured keratinocytes, topical application of DMBA to Bcl-x_L-deficient mice resulted in a significant, dose-dependent increase in the number of epidermal cells undergoing apoptosis compared with that in control mice, as analyzed by caspase-3 staining (Figure 5B; data shown for interfollicular epidermis only). As shown in Figure 5C, apoptotic cells were again observed in both the interfollicular epidermis and hair follicles. Similar to the results with UVB treatment, Bcl-x_L-deficient mice displayed a significantly elevated number of apoptotic cells at 24 and 48 hours after topical treatment with 100 nmol of DMBA in both the interfollicular epidermis as well as the hair follicles (Figure 5D and 5E, respectively). Analysis of caspase-3-stained cells in skin sections from

Bcl-x_L-deficient mice revealed that a greater proportion of the caspase-3-positive cells in epidermis of Bcl-x_L-deficient mice induced by DMBA treatment were localized in the hair follicles (Figures 5C and 5E). This is in contrast to the results with UVB-treated mice where a greater proportion of apoptotic cells was observed in the interfollicular epidermis as noted above. Nevertheless, in both cases there was an increase in apoptotic cells seen in the hair follicles of the Bcl-x_L-deficient mice. Similar to the results shown in Figures 2 and 3 for UVB treated mice, the apoptotic cells in the hair follicles appeared to reside in several different locations, including above the sebaceous glands and in the isthmus as well as the bulge region. The latter was assessed by confocal microscopy analysis and again showed that a proportion of the caspase-3 positive cells in the hair follicles induced by DMBA treatment also expressed K15 and/or CD34 and appeared to reside in the bulge region (data not shown). Collectively, these data indicate that Bcl-x_L plays a role in survival of keratinocytes, including stem/progenitor cells, following DNA damage induced by both UVB and DMBA.

Bcl-x_L deficiency does not influence epidermal proliferation induced by UVB irradiation or TPA treatment

In mouse skin, UVB irradiation causes an initial increase in apoptosis followed by keratinocyte proliferation and epidermal hyperplasia. To explore the impact of Bcl-x_L deficiency on this response, wild-type and Bcl-x_L-deficient mice were irradiated with a single dose of UVB at 1,200 J/m^2 and epidermal hyperplasia (as assessed by epidermal thickness) and cell proliferation (as assessed by BrdU labeling) were measured at 24 and 48 hours after exposure. Epidermal thickness was increased in both wild-type and Bcl-x_L-deficient mice in response to UVB irradiation, but no significant difference was found between genotypes at either timepoint (Figure 6A and B). Similarly, BrdU-positive cells were increased in the epidermis of both wild-type and Bcl-x_L-deficient mice 24 and 48 hours after UVB irradiation (Figure 6C). Again, no differences were seen between the two genotypes.

We also investigated the impact of Bcl-x_L deficiency on keratinocyte proliferation and epidermal hyperplasia induced by TPA. For these experiments, TPA was given as a single topical treatment of 6.8 nmol and mice were sacrificed 24 and 48 hours later. Keratinocyte proliferation and epidermal hyperplasia induced by TPA treatment were significantly increased in both wild-type and Bcl-x_L-deficient mice at 24 and 48 hours after TPA treatment (Figure 6D–F). Similar to the results obtained following UVB exposure, there were no differences seen in either epidermal hyperplasia (Figure 6E) or keratinocyte proliferation (Figure 6F) in Bcl-x_L-deficient versus wild-type mice following TPA treatment. Collectively, these results indicate that Bcl-x_L deficiency does not significantly affect epidermal cell proliferation or hyperplasia induced by either UVB irradiation or TPA treatment.

Impact of Bcl-x_L deficiency on both UVB and two-stage skin carcinogenesis

To further investigate the role of Bcl-x_L in skin carcinogenesis, wild-type and Bcl-x_L-deficient mice were subjected to either a UVB skin carcinogenesis protocol (Figure 7A and B) or a two-stage skin carcinogenesis protocol (Figure 7C and D). As shown in Figure 7A

and B, Bcl-x_L-deficient mice were less susceptible to skin carcinogenesis induced by UVB exposure compared to wild-type littermates. In this regard, the first skin tumor was observed in Bcl-x_L-deficient mice after 27 weeks of UVB irradiation, whereas wild-type mice started to develop skin tumors after 21 weeks of UVB irradiation. Ninety-five percent of wild-type mice developed tumors on the ear and back skin by the end of the experiment, whereas only 70% of the Bcl-x_L-deficient mice had developed tumors (Figure 7A). This difference was statistically significant after 15 weeks and for the remainder of the experiment. ($p < 0.05$, χ^2 test). Furthermore, the average number of skin tumors per mouse in Bcl-x_L-deficient mice was lower than in wild-type mice ($p < 0.05$ by Mann-Whitney U Test, Figure 7B). All tumors that developed in both types of mice were diagnosed as SCCs by the end of the observation period. Representative sections are shown in Figure 8A (top panel). In addition, immunohistochemical analyses showed Bcl-x_L expression in tumors from wild-type mice, but little or no expression in tumors from Bcl-x_L-deficient mice (again, see Figure 8A, bottom panels).

Similar results were obtained in a two-stage skin carcinogenesis experiment using DMBA as the initiator and TPA as the promoter. As shown in Figure 7C and D, Bcl-x_L-deficient mice were more resistant to two-stage skin carcinogenesis with reduced tumor formation when compared to wild-type littermates. In this regard, there was no significant difference in tumor incidence between wild-type and Bcl-x_L-deficient mice; i.e., 100% vs. 90%, respectively after 21 weeks of promotion with TPA (Figure 7C). However, there was a significant reduction in the average number of papillomas per mouse in Bcl-x_L-deficient mice compared to wild-type mice ($p < 0.05$ by Mann-Whitney U Test, Figure 7D).

Expression of antiapoptotic proteins is increased in the epidermis and skin tumors from Bcl-x_L-deficient mice

In addition to Bcl-x_L, the Bcl-2 family contains other survival factors, such as Bcl-2 and myeloid cell factor-1 (Mcl-1) [38]. Previous comparative studies have shown that apoptotic pathways inhibited by one antiapoptotic member can also be inhibited by other antiapoptotic members [2], indicating some degree of functional overlap allowing reciprocal regulation of cell survival. For example, it was shown that expression of a Bcl-x_L transgene was able to rescue Bcl-2 deficiency in mature T lymphocytes of Bcl-2-deficient mice [39]. Recent studies have also suggested that survivin, an important cell survival factor, is involved in skin carcinogenesis [40, 41]. During the initial characterization of skin-specific Bcl-x_L-deficient mice it was noted that Bcl-2 levels were significantly elevated [23]. To evaluate the levels of Bcl-2 and other antiapoptotic proteins in the epidermis of Bcl-x_L-deficient mice, Western blot analysis was performed using lysates prepared from epidermis and from skin tumors induced by either UVB irradiation or the DMBA/TPA two-stage protocol. As shown in Figure 8B, the levels of Bcl-2, Mcl-1, and survivin were higher in the epidermis of Bcl-x_L-deficient mice compared with wild-type mice. This was seen in the absence of any treatment. Notably, the levels of these three antiapoptotic proteins were also higher in skin tumors that developed in Bcl-x_L-deficient mice compared to wild-type mice regardless of the protocol used to induce the tumors (Figure 8C and D). These results suggest that increased expression of other antiapoptotic proteins may partially compensate for the loss of

Bcl-x_L expression in Bcl-x_L-deficient mice and this compensation may reduce the overall impact of Bcl-x_L deficiency on skin carcinogenesis.

Discussion

We have demonstrated that Bcl-x_L plays a role in skin carcinogenesis induced by both chemicals as well as UVB irradiation. In this regard, Bcl-x_L deficiency significantly increased sensitivity of mouse keratinocytes to both DMBA and UVB-induced apoptosis in culture as well as in mouse epidermis *in vivo*. In addition, increased sensitivity of follicular keratinocytes, including those located in stem/progenitor cell populations (which included those in the bulge region), was observed in Bcl-x_L-deficient mice after exposure to either DMBA or UVB irradiation. Further studies demonstrated that Bcl-x_L deficiency led to a more rapid loss of CPD-containing keratinocytes in epidermis *in vivo* consistent with the hypothesis that the antiapoptotic function of Bcl-x_L protects keratinocytes against DNA damage-induced apoptosis early after exposure to skin carcinogens. Bcl-x_L deficiency did not affect epidermal proliferation after exposure to either UVB or TPA suggesting little or no effect on the promotional phase of skin carcinogenesis. Finally, evaluation of the susceptibility of skin specific Bcl-x_L-deficient mice to skin carcinogenesis demonstrated reduced sensitivity to both two-stage DMBA/TPA and UVB-induced skin carcinogenesis. These results support the conclusion that Bcl-x_L is a Stat3 regulated gene that plays a role primarily during the initiation stage of epithelial carcinogenesis through its effects on survival of keratinocytes following DNA damage by DMBA or UVB irradiation.

In this study, we showed that Bcl-x_L deficiency in mice increased susceptibility of keratinocytes to both UVB- and DMBA-induced apoptosis. This increased sensitivity was seen both in cultured keratinocytes as well as in mouse epidermis *in vivo*. Previous studies from our laboratory showed that a significant proportion of apoptotic cells observed in Stat3-deficient mice following treatment with DMBA were localized in or near the bulge region of the hair follicles [26], suggesting that Stat3-mediated antiapoptotic gene regulation might be critical for maintaining the survival of bulge region KSCs after DMBA-induced DNA damage. Recent studies from our laboratory have also revealed that a significant number of apoptotic cells induced by UVB exposure in Stat3-deficient mice can be observed in or near the bulge region of the hair follicles [27]. In the current study, we also observed a proportion of apoptotic keratinocytes in the hair follicles. These apoptotic cells appeared to be located above the sebaceous glands, in a region between the sebaceous gland and the bulge region (called the isthmus) as well as in the bulge region of hair follicles in skin of both wild-type and Bcl-x_L-deficient mice following UVB irradiation (Figures 2 and 3) and treatment with DMBA (Figure 5 and data not shown). Bcl-x_L deficiency increased the overall incidence of apoptotic cells in these regions of the hair follicles.

Considerable evidence has accumulated implicating bulge region KSCs as targets for the development of skin tumors, especially with regard to two-stage chemical carcinogenesis [reviewed in 42, 43]. In addition, Nijhoff *et al.* [44] recently identified a novel murine progenitor cell population localized to a previously uncharacterized region above the bulge region. Cells in this region react with antibodies to the thymic epithelial progenitor marker MTS24. MTS24 positive cells do not express CD34 or K15 but possess a high proliferative

capacity similar to bulge region KSCs and may in fact be derived from the latter [44]. Furthermore, other stem/progenitor cells that do not express MTS24 or K15/CD34 may also reside in the same region called the upper isthmus [45]. Collectively, these data indicate that Bcl-x_L plays a role in survival of epidermal keratinocytes including those located in one or more hair follicle stem/progenitor cell compartment following DNA damage induced by either DMBA or UVB.

In the current study, we also examined the relationship between UV-photoproduct containing cells (i.e. CPD containing cells) and UVB-induced apoptosis *in vivo* following UVB irradiation. Recently, Nijhoff *et al.* [46] reported that UV-photoproducts (CPDs and 6-4 PPs) accumulated in epidermal basal cells including putative stem/progenitor cells following chronic UVB exposure to skin of SkH-1 hairless mice. Furthermore, we have recently found that keratinocytes containing both 6-4 PPs and CPDs can be observed in the interfollicular epidermis as well as hair follicles after only a single exposure to UVB [27]. In addition, in our previous study UV-photoproduct containing cells in the hair follicles appeared to persist longer than those in the interfollicular epidermis. Furthermore, we found that UV-photoproduct containing cells disappeared faster from Stat3-deficient mice compared to wild-type and K5.Stat3C transgenic mice. As shown in Figure 4 of the current study, we found that Bcl-x_L deficiency led to a more rapid disappearance of CPD-containing keratinocytes. This was true for CPD containing cells located in both the interfollicular epidermis and hair follicles (data not shown). These data further support the hypothesis that Bcl-x_L may mediate, at least in part, some of the effects of Stat3 during the initiation of epithelial carcinogenesis.

We also examined whether Bcl-x_L deficiency impacted epidermal proliferation following exposure to either UVB or TPA. Pena *et al.* [24] previously reported that overexpression of Bcl-x_L under control of the K14 promoter did not affect cell proliferation or differentiation in the epidermis. In addition, expression of the Bcl-x_L transgene did not affect wound healing. As shown in Figure 6 of the current study, Bcl-x_L deficiency did not impact epidermal hyperplasia or cell proliferation following either UVB irradiation or TPA treatment. Thus, unlike Stat3, which regulates a number of critical cell cycle regulatory genes (e.g., cyclin D1, c-myc, etc.) [47, 48] involved in epidermal proliferation following UVB or TPA treatment, Bcl-x_L does not affect these pathways or epidermal proliferation. The current data indicate a primary role of Bcl-x_L in epithelial carcinogenesis during early events related to the initiation of tumors through effects on keratinocyte (including stem/progenitor cell) survival following DNA damage.

Evaluation of the susceptibility of Bcl-x_L-deficient mice to carcinogenesis induced by either a UVB or DMBA/TPA protocol demonstrated that they were moderately resistant to skin tumor formation compared with control littermates (Figure 7). However, inhibition of tumor formation observed in Bcl-x_L-deficient mice was not as dramatic as that observed in Stat3-deficient mice [26, 27]. In this regard, skin-specific Stat3-deficient mice were completely resistant to two-stage (DMBA/TPA) skin carcinogenesis. Furthermore, very recently we employed an inducible system to specifically delete Stat3 at the time of initiation or during promotion [31]. Deletion of Stat3 at the time of initiation led to a significant reduction in papilloma formation. Thus, the overall impact of Bcl-x_L deficiency on skin carcinogenesis

induced by both two-stage and UVB protocol is less than observed with Stat3 deficiency. This is likely due to several mechanisms. First, Stat3 increases both cell survival and proliferation through its transcriptional regulation of multiple genes as noted above, whereas Bcl-x_L appears to have an impact primarily on keratinocyte survival. Second, Stat3 increases cell survival by regulating a series of antiapoptotic proteins, whereas Bcl-x_L is one of a family of antiapoptotic proteins regulated by Stat3. Thus, other antiapoptotic proteins regulated by Stat3 may compensate for the loss of Bcl-x_L expression through redundant functions. As noted in the Introduction, evidence suggests that Bcl-2 and survivin play a role in mouse skin carcinogenesis [17, 18, 40] through their functions as antiapoptotic proteins. Bcl-2, survivin and Mcl-1 are known to be regulated by Stat3 [49–51]. Consistent with this idea, levels of Bcl-2, Mcl-1, and survivin were increased in the epidermis and in skin tumors of Bcl-x_L-deficient mice compared with control littermates (Figure 8). Therefore, elevated levels of one or more of these proteins may function to limit the impact of Bcl-x_L loss in keratinocytes.

Finally, we reported that overexpression of a constitutively active form of Stat3 (i.e., Stat3C) under control of the bovine K5 promoter enhanced susceptibility to two-stage DMBA/TPA skin carcinogenesis [52] as well as UVB skin carcinogenesis [27]. In the course of these studies, we noted that elevated Stat3 activity in the epidermis of these mice significantly enhanced malignant progression. In fact, by 20 weeks of promotion with TPA essentially all tumors in a two-stage skin carcinogenesis protocol were diagnosed as SCCs. Pena *et al*. [25] reported that overexpression of Bcl-x_L in epidermis enhanced malignant conversion during a two-stage DMBA/TPA skin carcinogenesis protocol. Thus, the possibility exists that elevated Bcl-x_L levels that occur in epidermis of Stat3C mice [27] might contribute to the enhanced tumor progression seen in these mice. Ongoing experiments are further exploring this possibility using a system to inducibly delete Bcl-x_L in papillomas as we have recently described for inducible deletion of Stat3 [31].

In conclusion, Bcl-x_L appears to play a significant role in skin carcinogenesis through its effects on survival of DNA-damaged keratinocytes. The current studies focused on early events associated with both chemically-induced as well as UVB-induced carcinogenesis. The ability of Bcl-x_L to protect keratinocytes, including putative stem/progenitor cells (e.g., bulge region KSCs) implies a major role in the initiation phase of skin tumor development. Bcl-x_L may mediate some of the effects of Stat3 during epithelial carcinogenesis and may represent a novel target for cancer prevention as recently suggested [9].

Acknowledgments

This work was supported by NCI grants CA76520, CA105345, University of Texas M.D. Anderson Cancer Center Support Grant CA16672, and National Institute of Environmental Health Sciences Center Grant ES07784. Funding as an Odyssey Fellow was supported by the Odyssey Program and The H-E-B Award for Scientific Achievement at The University of Texas M.D. Anderson Cancer Center (to D. J. Kim). We also thank Shawna Johnson and Linda Beltrán for their assistance in the preparation of this manuscript.

Abbreviations used

Stat3 signal transducer and activator of transcription 3

UVB	ultraviolet B
K5	keratin 5
DMBA	7,12-dimethylbenz[*a*]anthracene
TPA	12-*O*-tetradecanoylphorbol-13-acetate
Bcl-2	B-cell lymphoma-2
PI3K	phosphatidylinositol-3-kinase
SCC	squamous cell carcinoma
KSCs	keratinocyte stem cells
RNAi	RNA interference
siRNA	short interfering RNA
FACS	fluorescence-activated cell sorting
CPD	cyclobutane pyrimidine dimer
BrdU	5-bromo-2-deoxyuridine
6-4PP	pyrimidine (6-4) pyrimidone photoproduct
Mcl-1	myeloid cell factor-1

References

1. Edinger AL, Thompson CB. Death by design: apoptosis, necrosis and autophagy. Curr Opin Cell Biol. 2004; 16(6):663–669. [PubMed: 15530778]
2. Strasser A, O'Connor L, Dixit VM. Apoptosis signaling. Annu Rev Biochem. 2000; 69:217–245. [PubMed: 10966458]
3. Danial NN, Korsmeyer SJ. Cell death: critical control points. Cell. 2004; 116(2):205–219. [PubMed: 14744432]
4. Chao DT, Korsmeyer SJ. BCL-2 family: regulators of cell death. Annu Rev Immunol. 1998; 16:395–419. [PubMed: 9597135]
5. Reed JC. Dysregulation of apoptosis in cancer. J Clin Oncol. 1999; 17(9):2941–2953. [PubMed: 10561374]
6. Rudin CM, Thompson CB. Apoptosis and disease: regulation and clinical relevance of programmed cell death. Annu Rev Med. 1997; 48:267–281. [PubMed: 9046961]
7. Thompson CB. Apoptosis in the pathogenesis and treatment of disease. Science. 1995; 267(5203): 1456–1462. [PubMed: 7878464]
8. Youle RJ, Strasser A. The BCL-2 protein family: opposing activities that mediate cell death. Nat Rev Mol Cell Biol. 2008; 9(1):47–59. [PubMed: 18097445]
9. Zhang J, Bowden GT. Targeting Bcl-X(L) for prevention and therapy of skin cancer. Molecular carcinogenesis. 2007; 46(8):665–670. [PubMed: 17443741]
10. Tu Y, Renner S, Xu F, et al. BCL-X expression in multiple myeloma: possible indicator of chemoresistance. Cancer research. 1998; 58(2):256–262. [PubMed: 9443402]
11. Zapata JM, Krajewska M, Krajewski S, et al. Expression of multiple apoptosis-regulatory genes in human breast cancer cell lines and primary tumors. Breast Cancer Res Treat. 1998; 47(2):129–140. [PubMed: 9497101]

12. McConkey DJ, Greene G, Pettaway CA. Apoptosis resistance increases with metastatic potential in cells of the human LNCaP prostate carcinoma line. Cancer research. 1996; 56(24):5594–5599. [PubMed: 8971161]
13. Nunez G, London L, Hockenbery D, Alexander M, McKearn JP, Korsmeyer SJ. Deregulated Bcl-2 gene expression selectively prolongs survival of growth factor-deprived hemopoietic cell lines. J Immunol. 1990; 144(9):3602–3610. [PubMed: 2184193]
14. McDonnell TJ, Troncoso P, Brisbay SM, et al. Expression of the protooncogene bcl-2 in the prostate and its association with emergence of androgen-independent prostate cancer. Cancer research. 1992; 52(24):6940–6944. [PubMed: 1458483]
15. Lu QL, Elia G, Lucas S, Thomas JA. Bcl-2 proto-oncogene expression in Epstein-Barr-virus-associated nasopharyngeal carcinoma. Int J Cancer. 1993; 53(1):29–35. [PubMed: 8380056]
16. Pezzella F, Turley H, Kuzu I, et al. bcl-2 protein in non-small-cell lung carcinoma. N Engl J Med. 1993; 329(10):690–694. [PubMed: 8393963]
17. Rodriguez-Villanueva J, Greenhalgh D, Wang XJ, et al. Human keratin-1.bcl-2 transgenic mice aberrantly express keratin 6, exhibit reduced sensitivity to keratinocyte cell death induction, and are susceptible to skin tumor formation. Oncogene. 1998; 16(7):853–863. [PubMed: 9484776]
18. Rossiter H, Beissert S, Mayer C, et al. Targeted expression of bcl-2 to murine basal epidermal keratinocytes results in paradoxical retardation of ultraviolet- and chemical-induced tumorigenesis. Cancer Research. 2001; 61(9):3619–3626. [PubMed: 11325830]
19. Dai Y, Grant S. Targeting multiple arms of the apoptotic regulatory machinery. Cancer research. 2007; 67(7):2908–2911. [PubMed: 17409392]
20. Zhang YL, Pang LQ, Wu Y, Wang XY, Wang CQ, Fan Y. Significance of Bcl-xL in human colon carcinoma. World J Gastroenterol. 2008; 14(19):3069–3073. [PubMed: 18494061]
21. Adams JM, Cory S. The Bcl-2 apoptotic switch in cancer development and therapy. Oncogene. 2007; 26(9):1324–1337. [PubMed: 17322918]
22. Taylor JK, Zhang QQ, Monia BP, Marcusson EG, Dean NM. Inhibition of Bcl-xL expression sensitizes normal human keratinocytes and epithelial cells to apoptotic stimuli. Oncogene. 1999; 18(31):4495–4504. [PubMed: 10442640]
23. Umeda J, Sano S, Kogawa K, et al. In vivo cooperation between Bcl-xL and the phosphoinositide 3-kinase-Akt signaling pathway for the protection of epidermal keratinocytes from apoptosis. Faseb J. 2003; 17(6):610–620. [PubMed: 12665473]
24. Pena JC, Fuchs E, Thompson CB. Bcl-x expression influences keratinocyte cell survival but not terminal differentiation. Cell Growth Differ. 1997; 8(6):619–629. [PubMed: 9185996]
25. Pena JC, Rudin CM, Thompson CB. A Bcl-xL transgene promotes malignant conversion of chemically initiated skin papillomas. Cancer research. 1998; 58(10):2111–2116. [PubMed: 9605754]
26. Chan KS, Sano S, Kiguchi K, et al. Disruption of Stat3 reveals a critical role in both the initiation and the promotion stages of epithelial carcinogenesis. J Clin Invest. 2004; 114(5):720–728. [PubMed: 15343391]
27. Kim DJ, Angel J, Sano S, DiGiovanni J. Constitutive activation and targeted disruption of signal transducer and activator of transcription 3 (Stat3) in mouse epidermis reveal its critical role in UVB-induced skin carcinogenesis. Oncogene. 2008 In press.
28. Sano S, Chan KS, Kira M, et al. Signal transducer and activator of transcription 3 is a key regulator of keratinocyte survival and proliferation following UV irradiation. Cancer research. 2005; 65(13): 5720–5729. [PubMed: 15994947]
29. Grad JM, Zeng XR, Boise LH. Regulation of Bcl-xL: a little bit of this and a little bit of STAT. Curr Opin Oncol. 2000; 12(6):543–549. [PubMed: 11085453]
30. Grillot DA, Gonzalez-Garcia M, Ekhterae D, et al. Genomic organization, promoter region analysis, and chromosome localization of the mouse bcl-x gene. J Immunol. 1997; 158(10):4750–4757. [PubMed: 9144489]
31. Kataoka K, Kim DJ, Carbajal S, Clifford J, DiGiovanni J. Stage-specific disruption of Stat3 demonstrates a direct requirement during both the initiation and promotion stages of mouse skin tumorigenesis. Carcinogenesis. 2008; 29:1108–1114. [PubMed: 18453544]

32. Dlugosz AA, Glick AB, Tennenbaum T, Weinberg WC, Yuspa SH. Isolation and utilization of epidermal keratinocytes for oncogene research. Methods Enzymol. 1995; 254:3–20. [PubMed: 8531694]
33. Trempus CS, Morris RJ, Bortner CD, et al. Enrichment for living murine keratinocytes from the hair follicle bulge with the cell surface marker CD34. The Journal of investigative dermatology. 2003; 120(4):501–511. [PubMed: 12648211]
34. Noonan FP, Otsuka T, Bang S, Anver MR, Merlino G. Accelerated ultraviolet radiation-induced carcinogenesis in hepatocyte growth factor/scatter factor transgenic mice. Cancer research. 2000; 60(14):3738–3743. [PubMed: 10919643]
35. Setlow RB, Carrier WL. Pyrimidine dimers in ultraviolet-irradiated DNA's. J Mol Biol. 1966; 17(1):237–254. [PubMed: 4289765]
36. Lippke JA, Gordon LK, Brash DE, Haseltine WA. Distribution of UV light-induced damage in a defined sequence of human DNA: detection of alkaline-sensitive lesions at pyrimidine nucleoside-cytidine sequences. Proc Natl Acad Sci U S A. 1981; 78(6):3388–3392. [PubMed: 6943547]
37. Mitchell DL, Nairn RS. The biology of the (6-4) photoproduct. Photochem Photobiol. 1989; 49(6): 805–819. [PubMed: 2672059]
38. Adams JM, Cory S. The Bcl-2 protein family: arbiters of cell survival. Science. 1998; 281(5381): 1322–1326. [PubMed: 9735050]
39. Chao DT, Linette GP, Boise LH, White LS, Thompson CB, Korsmeyer SJ. Bcl-XL and Bcl-2 repress a common pathway of cell death. J Exp Med. 1995; 182(3):821–828. [PubMed: 7650488]
40. Zhang W, Hanks AN, Boucher K, et al. UVB-induced apoptosis drives clonal expansion during skin tumor development. Carcinogenesis. 2005; 26(1):249–257. [PubMed: 15498793]
41. Allen SM, Florell SR, Hanks AN, et al. Survivin expression in mouse skin prevents papilloma regression and promotes chemical-induced tumor progression. Cancer research. 2003; 63(3):567–572. [PubMed: 12566297]
42. Trempus CS, Morris RJ, Ehinger M, et al. CD34 expression by hair follicle stem cells is required for skin tumor development in mice. Cancer research. 2007; 67(9):4173–4181. [PubMed: 17483328]
43. Kangsamaksin T, Park HJ, Trempus CS, Morris RJ. A perspective on murine keratinocyte stem cells as targets of chemically induced skin cancer. Molecular Carcinogenesis. 2007; 46(8):579–584. [PubMed: 17583566]
44. Nijhof JG, Braun KM, Giangreco A, et al. The cell-surface marker MTS24 identifies a novel population of follicular keratinocytes with characteristics of progenitor cells. Development (Cambridge, England). 2006; 133(15):3027–3037.
45. Jensen UB, Yan X, Triel C, Woo SH, Christensen R, Owens DM. A distinct population of clonogenic and multipotent murine follicular keratinocytes residing in the upper isthmus. Journal of Cell Science. 2008; 121(Pt 5):609–617. [PubMed: 18252795]
46. Nijhof JG, van Pelt C, Mulder AA, Mitchell DL, Mullenders LH, de Gruijl FR. Epidermal stem and progenitor cells in murine epidermis accumulate UV damage despite NER proficiency. Carcinogenesis. 2007; 28(4):792–800. [PubMed: 17127714]
47. Dauer DJ, Ferraro B, Song L, et al. Stat3 regulates genes common to both wound healing and cancer. Oncogene. 2005; 24(21):3397–3408. [PubMed: 15735721]
48. Bromberg JF. Activation of STAT proteins and growth control. Bioessays. 2001; 23(2):161–169. [PubMed: 11169589]
49. Epling-Burnette PK, Liu JH, Catlett-Falcone R, et al. Inhibition of STAT3 signaling leads to apoptosis of leukemic large granular lymphocytes and decreased Mcl-1 expression. J Clin Invest. 2001; 107(3):351–362. [PubMed: 11160159]
50. Gritsko T, Williams A, Turkson J, et al. Persistent activation of stat3 signaling induces survivin gene expression and confers resistance to apoptosis in human breast cancer cells. Clin Cancer Res. 2006; 12(1):11–19. [PubMed: 16397018]
51. Catlett-Falcone R, Landowski TH, Oshiro MM, et al. Constitutive activation of Stat3 signaling confers resistance to apoptosis in human U266 myeloma cells. Immunity. 1999; 10(1):105–115. [PubMed: 10023775]

52. Chan KS, Sano S, Kataoka K, et al. Forced expression of a constitutively active form of Stat3 in mouse epidermis enhances malignant progression of skin tumors induced by two-stage carcinogenesis. Oncogene. 2008; 27(8):1087–1094. [PubMed: 17700521]

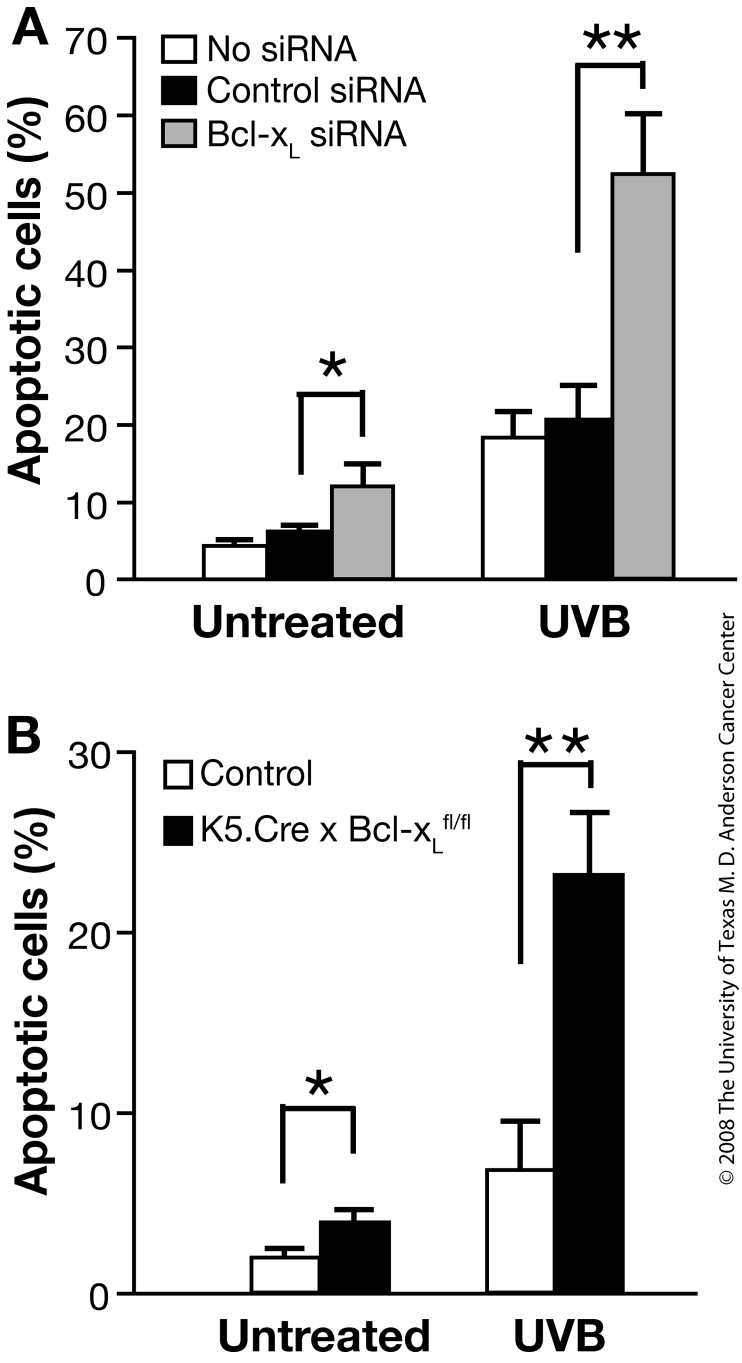

Fig. 1. Response of Bcl-x_L-deficient keratinocytes to UVB-induced apoptosis *in vitro*

(A) Percentage of apoptotic cells in keratinocytes irradiated by UVB at 800 J/m^2 after inhibition of Bcl-x_L expression by siRNA. DNA strand breaks were quantified in individual keratinocytes by fluorescence microscopy 12 hours after UVB irradiation. (B) Percentage of apoptotic cells in control and Bcl-x_L-deficient cultured keratinocytes after UVB irradiation as assessed by FACS analysis. Apoptotic cells were defined as the relative sub-G_1 population 12 hours after UVB irradiation. *$P < 0.05$ and **$P < 0.01$, Mann-Whitney *U* test.

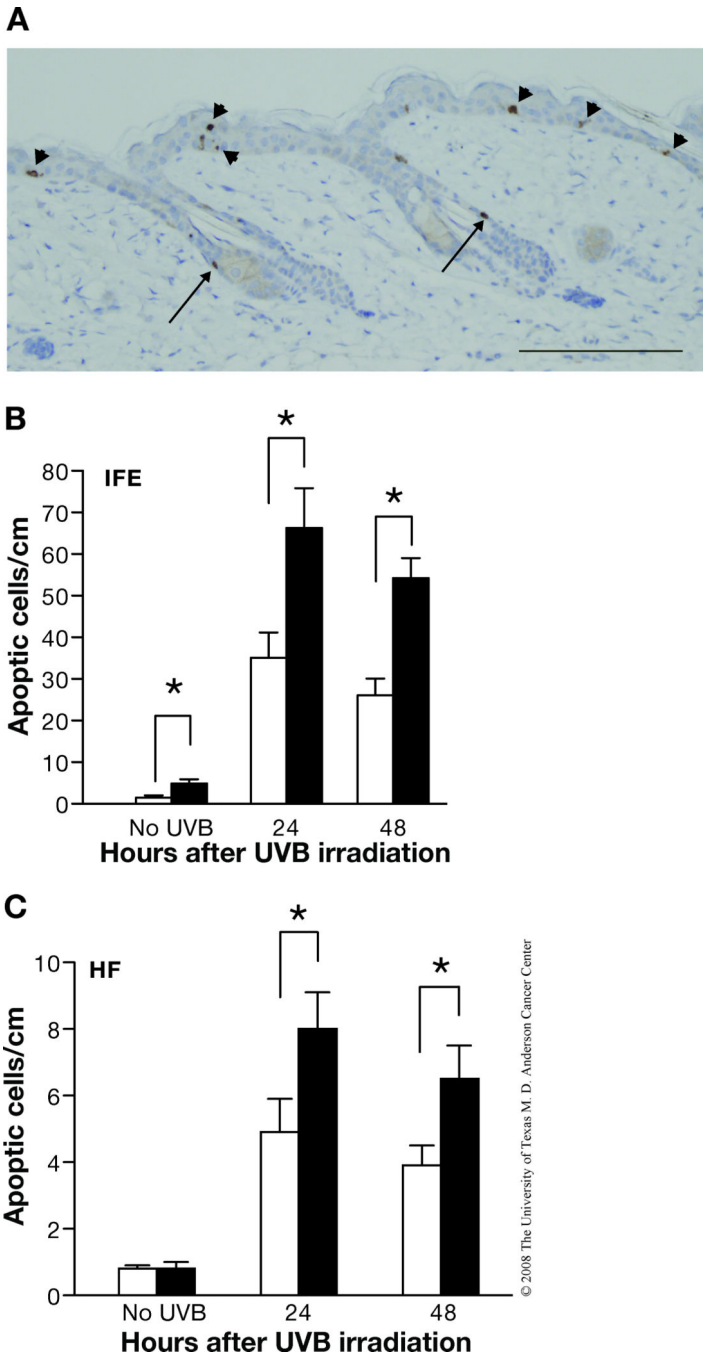

Fig. 2. Response of Bcl-x_L-deficient keratinocytes to UVB-induced apoptosis *in vivo*

(A) Representative caspase-3 staining of epidermis from Bcl-x_L-deficient mice after UVB irradiation. Scale bar: 20 μm. (B–C) Quantitation of the number of caspase-3-positive cells per centimeter of epidermis from wild-type and Bcl-x_L-deficient mice after UVB irradiation. Groups of mice (n = 3) were irradiated at 1,200 J/m^2 and sacrificed 24 or 48 hours after irradiation. *$P < 0.05$ and **$P < 0.01$ by Mann-Whitney *U* test. (B) Interfollicular epidermis (IFE). (C) Hair follicles (HF)

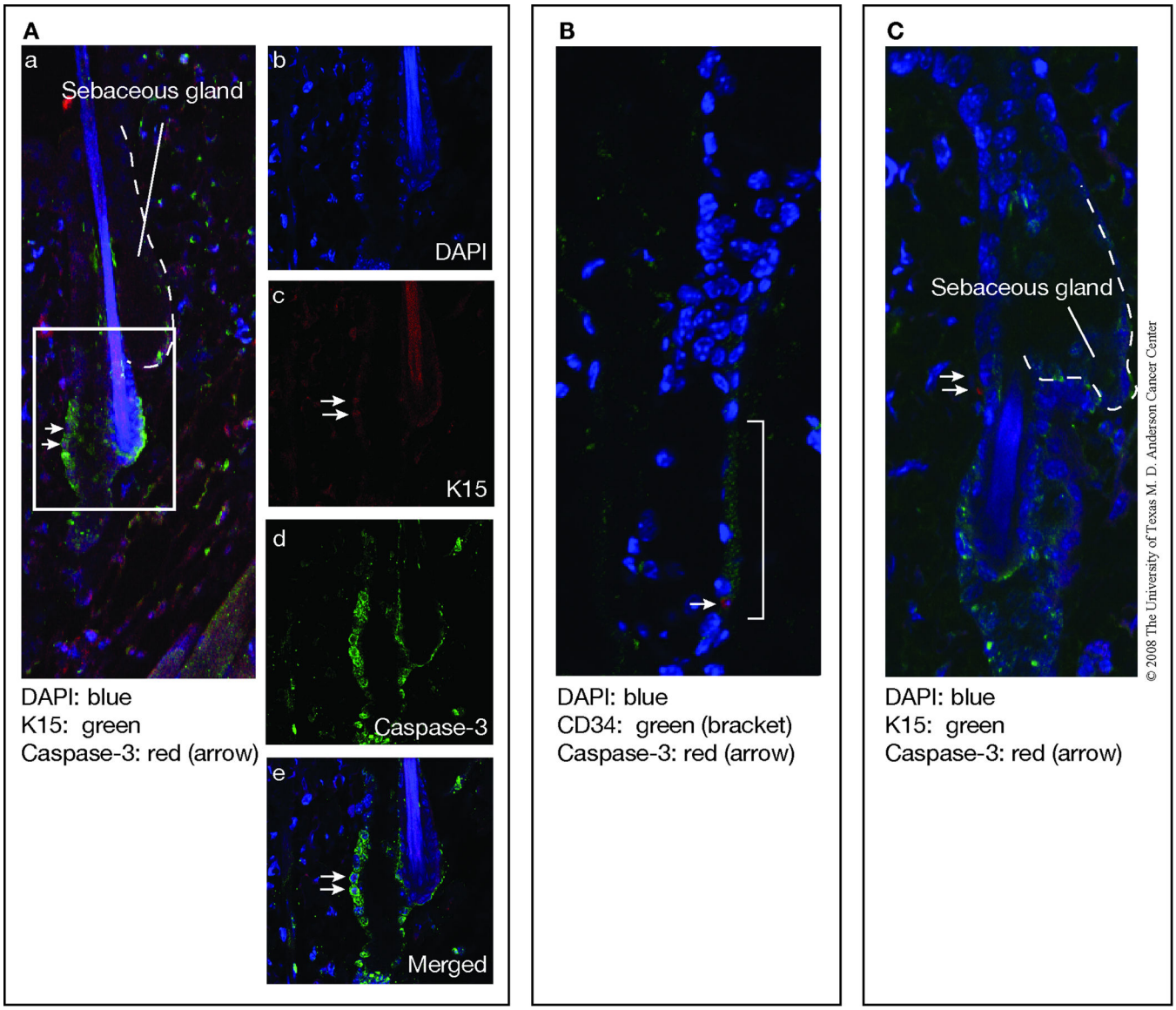

Fig. 3. Co-localization of K15 or CD34 and active caspase-3 in bulge region keratinocytes of K5.Cre × Bcl-x_L $^{fl/fl}$ mice

Mice were irradiated at 1,200 J/m^2 and sacrificed 24 hours after irradiation. (A) Left panel (a) shows a wide view of the skin section with merged images of DAPI (blue), K15 (green), and caspase-3 (red). The skin section contains two adjacent hair follicles. The right hair follicle has a hair shaft and a sebaceous gland while the left hair follicle is a follicle in telogen phase with bulge region keratinocytes that stained positive for K15 (green) and caspase-3 (red) (marked with arrows). Magnified views of the selected section in the left panel (area bordered by white rectangle) are shown in panels b (DAPI), c (K15), d (caspase-3) and e (merged). (B) Merged images of DAPI (blue), CD34 (green, bracketed), and caspase-3 (red). The arrow indicates a keratinocyte that is positive for both CD34 and caspase-3, which is located in the bulge region of the hair follicle. (C) Merged images of DAPI (blue), K15 (green), and caspase-3 (red). The arrows indicate keratinocytes that are

positive for caspase-3 but are localized in the area above the bulge region of the hair follicles.

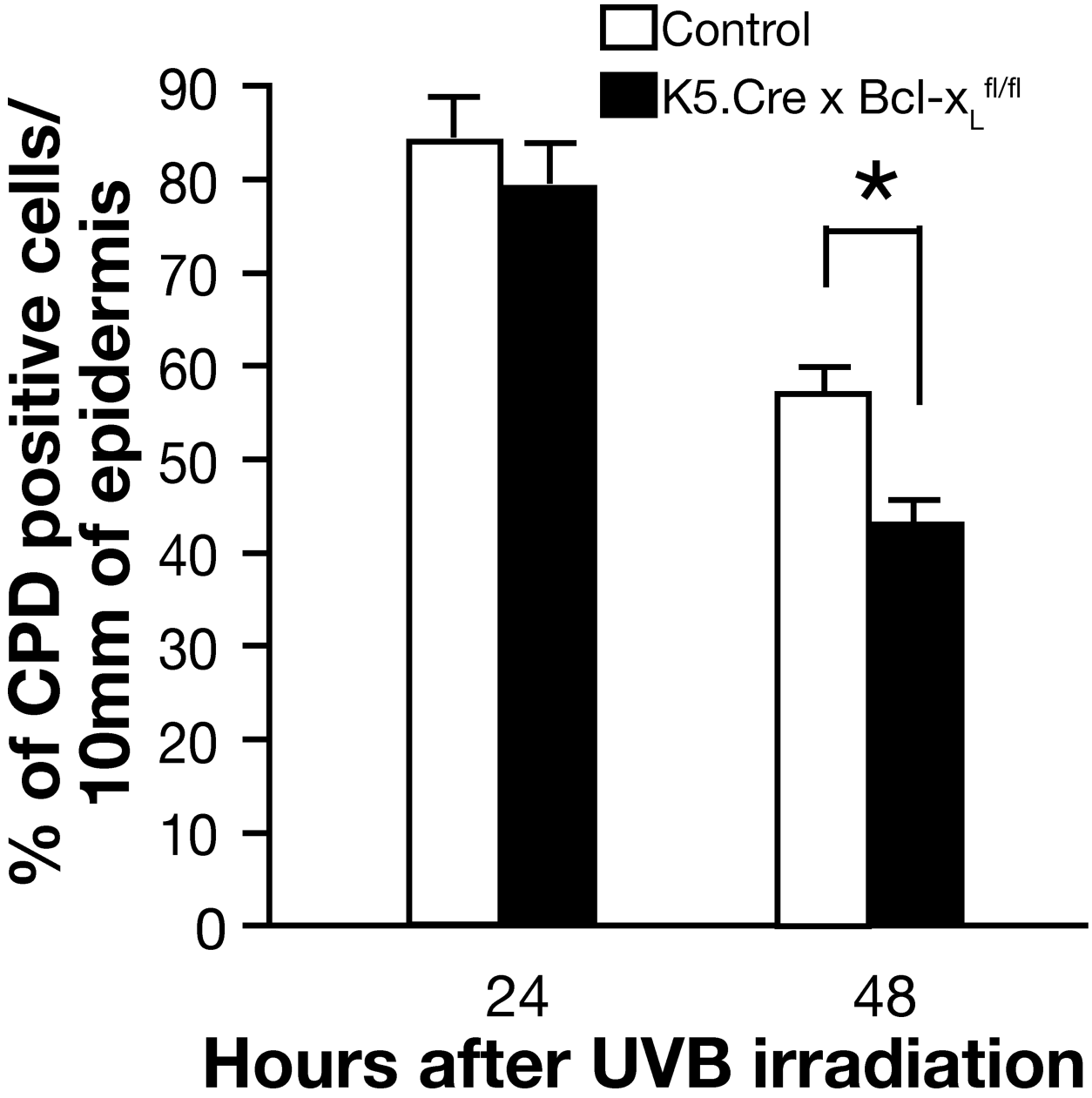

Fig. 4. Impact of Bcl-x_L-deficiency on levels of CPD-containing keratinocytes

Groups of mice (n=3) were irradiated with 1,200 J/m^2 and sacrificed 24 and 48 h after UVB exposure. Data shown are percentage of CPD-positive cells per 10 millimeters of epidermis and include CPD positive cells from both the interfollicular epidermis and hair follicles of control (wild-type) and Bcl-x_L-deficient mice). *$P < 0.05$ by Mann-Whitney *U* test.

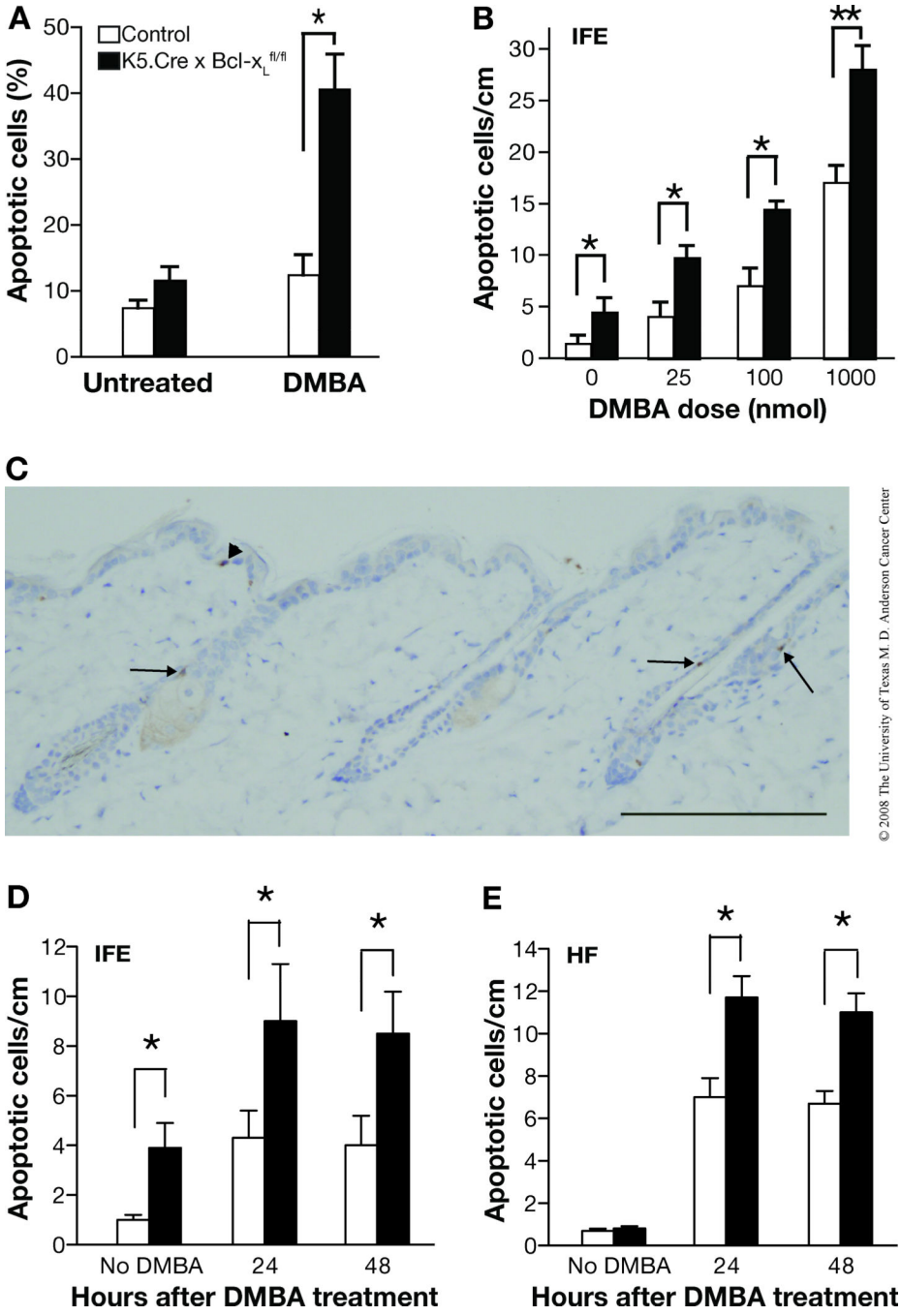

Fig. 5. Response of Bcl-x_L-deficient keratinocytes to DMBA-induced apoptosis both *in vitro* and *in vivo*

(A) Quantitation of apoptotic cells in cultured keratinocytes derived from control (wild-type) and Bcl-x_L-deficient mice following a single treatment of DMBA at a final concentration of 30 nM. Cell morphology was evaluated 12 hours after treatment. (B) Apoptotic index was assessed by determination of the number of caspase-3-positive cells per centimeter of interfollicular epidermis (IFE) in wild-type and Bcl-x_L-deficient mice after treatment with DMBA. *$P < 0.05$ and **$P < 0.01$ by Mann-Whitney *U* test. Groups of mice (n = 3) received a single topical treatment of DMBA at the indicated doses and were sacrificed 24

hours after treatment. (C) Representative section of caspase-3 staining of epidermis from Bcl-x_L-deficient mice 24 hours after DMBA treatment. Scale bar: 20 μm. (D–E) Groups of mice (n = 3) received a single topical dose of 100 nmol of DMBA and were sacrificed either 24 or 48 hours after treatment. (D) Interfollicular epidermis (IFE). (E) Hair follicles (HF). *$P < 0.05$ by Mann-Whitney U test.

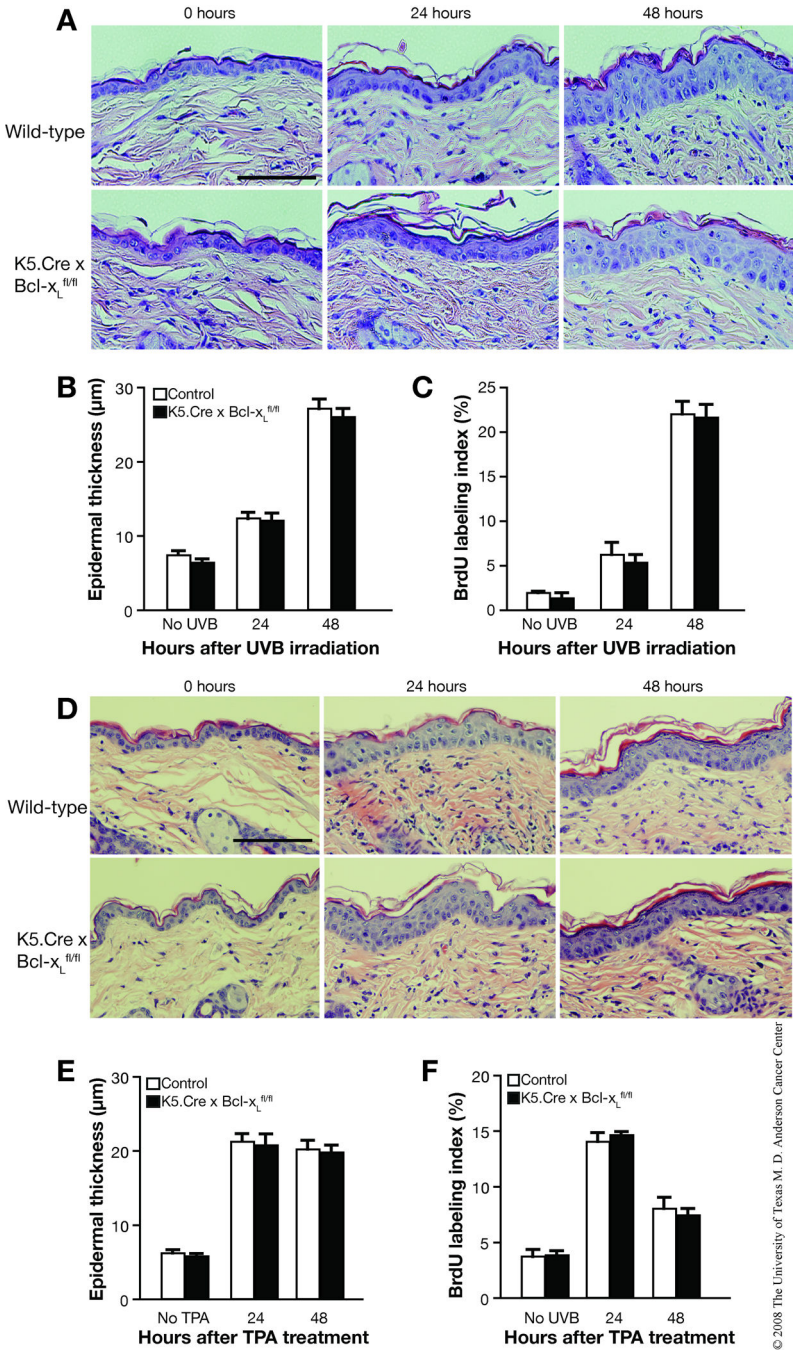

Fig. 6. Impact of Bcl-x_L on UVB- and TPA-induced epidermal hyperproliferation

(A–C) Groups of mice (n = 3) were irradiated with a single dose of UVB of 1,200 J/m^2 and were sacrified 24 or 48 hours after irradiation. (A) Representative hematoxylin and eosin (H and E) staining of the epidermis from wild-type and Bcl-x_L-deficient mice. Scale bar: 50 μm. (B) Quantification of epidermal thickness in skin sections from wild-type and Bcl-x_L-deficient mice irradiated by UVB. (C) Quantification of BrdU-positive cells from the epidermis of wild-type and Bcl-x_L-deficient mice after UVB irradiation. (D–F) Groups of mice (n = 3) were treated topically with a single application of TPA and sacrificed 24 or 48

hours after treatment. (D) Representative H and E staining of the epidermis from wild-type and Bcl-x_L-deficient mice. Scale bar: 50 μm. (E) Quantification of epidermal thickness in skin sections from wild-type and Bcl-x_L-deficient mice following treatment with TPA. (F) Quantification of BrdU-positive cells in the epidermis of wild-type and Bcl-x_L-deficient mice after treatment with TPA.

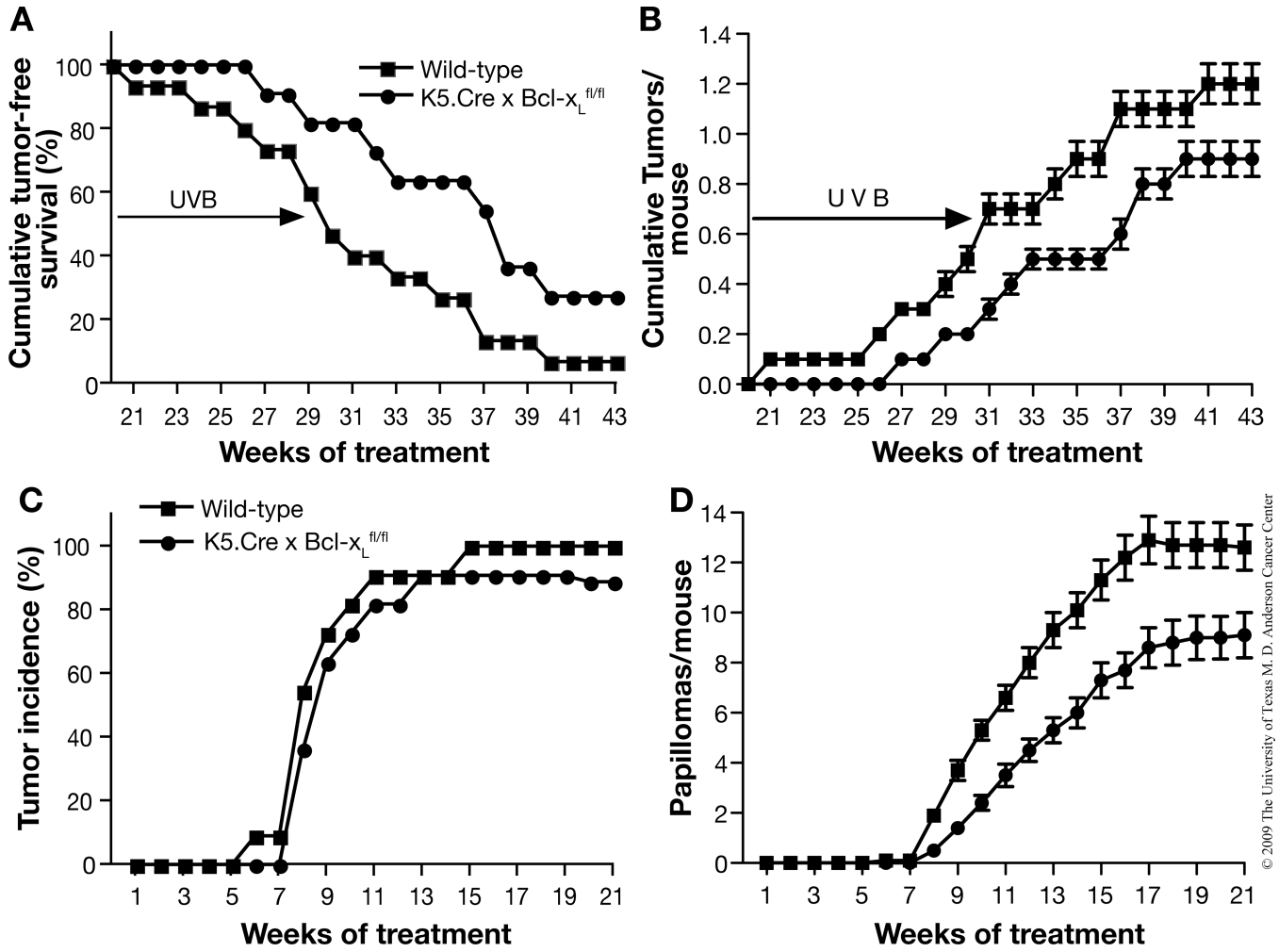

Fig. 7. Responsiveness of Bcl-x_L-deficient mice to both UVB- and chemically-induced skin carcinogenesis

(A and B) Groups of mice (wild-type, n=15; Bcl-x_L-deficient, n=11) were exposed to UVB three times a week for 30 weeks. (A) Percentage of mice without skin tumors. (B) Average number of skin tumors per mouse (the mean±s.e.m). (C and D) Groups of mice (wild-type, n=11; Bcl-x_L-deficient, n=11) were initiated with 25 nmol of DMBA and, after two weeks, were treated with twice-weekly applications of 6.8 nmol TPA for the duration of the experiment. (C) Percentage of mice without skin tumors. (D) Average number of skin tumors per mouse (the mean±s.e.m.).

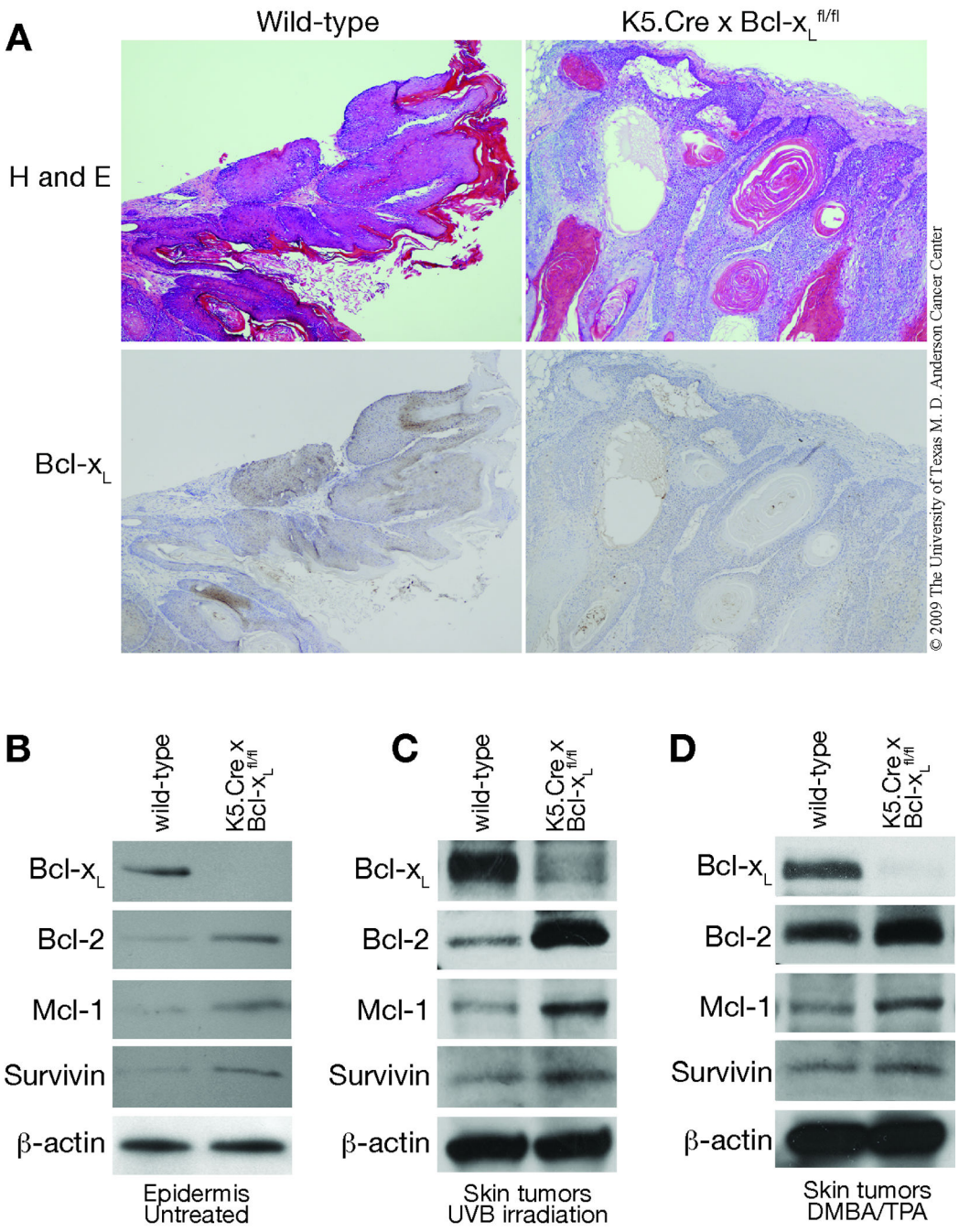

Fig. 8. Comparison of expression of antiapoptotic proteins in the epidermis and skin tumors of wild-type and Bcl-x_L-deficient mice

(A, top panels) Hematoxylin and eosin (H and E) stained sections of representative skin tumors. (A, bottom panels) Immunohistochemical staining of Bcl-x_L in these same skin tumors. Scale bar: 20 μm (B) Western blot analysis of Bcl-x_L and other antiapoptotic proteins in untreated epidermis from wild-type and Bcl-x_L-deficient mice. (C) Western blot analysis of Bcl-x_L and other antiapoptotic proteins in skin tumors from wild-type and Bcl-x_L-deficient mice induced by UVB irradiation. (D) Western blot analysis of Bcl-x_L and other antiapoptotic proteins in skin tumors from wild-type and Bcl-x_L-deficient mice

induced by the DMBA/TPA protocol. Protein lysates were prepared from epidermis and from pooled skin tumors and subjected to Western blot analysis. β-actin was used to standardize protein loading.